Eur. Phys. J. D **9**, 289–295 (1999)

THE EUROPEAN PHYSICAL JOURNAL D

EDP Sciences

Ionization potentials of hypervalent Li_nC ($2 \leq n \leq 10$)

P. Lievens[1,a], P. Thoen[1], S. Bouckaert[1], W. Bouwen[1], F. Vanhoutte[1], H. Weidele[1], R.E. Silverans[1], A. Navarro-Vázquez[2,b], and P.v.R. Schleyer[2,3]

[1] Laboratorium voor Vaste-Stoffysica en Magnetisme, K.U. Leuven, B-3001 Leuven, Belgium
[2] Computer Chemistry Center, Institut für Organische Chemie, Universität Erlangen-Nürnberg, D-91054 Erlangen, Germany
[3] Computer Chemistry Annex, University of Georgia, Athens, GA 30602-2525, USA

Received: 1 September 1998 / Received in final form: 9 December 1998

Abstract. We report on a combined experimental and theoretical investigation of the ionization potentials of small lithium monocarbide clusters. The clusters were produced by a laser vaporization source, and their ionization potentials were measured by threshold photoionization spectroscopy. The structures of the smaller clusters ($n \leq 8$), which are governed by hypervalent (hyperlithiated) bonding mechanisms, were calculated by means of density functional theory. Vertical and adiabatic ionization potentials were computed and compared with the experimental data.

PACS. 36.40.Vz Optical properties of clusters – 33.80.Eh Autoionization, photoionization, and photodetachment

1 Introduction

Since the experimental discovery and the theoretical verification, twenty years ago, of 'hyperlithiated' bonding, which involves formal violations of the octet rule in doped Li clusters [1, 2], there have been extensive theoretical and experimental investigations with the purpose of obtaining more evidence and insight in the specific structural and electronic properties of these systems [3–11]. One particularly interesting cluster is octahedral Li_6C, which possesses two valence electrons in excess of a filled octet around the C atom. Despite this, Li_6C was first predicted [3] and later verified experimentally [12] to be stable with respect to dissociation into the stoichiometric Li_4C and Li_2 molecules. Although many hypervalent clusters have now been described computationally, very little experimental information on their properties exists.

We report here on a combined experimental and theoretical investigation of the structures and ionization potentials (IPs) of small Li_nC clusters. The structures of Li_nC and Li_nC^+ clusters ($n \leq 8$) were computed by employing density functional theory [13]. Adiabatic and vertical IPs are deduced and compared with experiment. Threshold photoionization spectroscopy was performed on Li clusters doped with C or O. The experimental determination of the IP of Li_nO ($2 \leq n \leq 70$) compared with density functional theory (DFT) calculations on the small clusters ($n \leq 8$) is reported elsewhere [14], as is a discussion on the metallic properties of larger Li_nO and Li_nC clusters [15].

2 Experiments

The experimental setup and procedure is very similar to the one described in references [14–16] and will be discussed only briefly. The clusters, produced by a laser vaporization source with enriched ^{7}Li as target material, were laser-ionized, mass-selected, and detected in a reflectron time-of-flight mass spectrometer. The most abundant clusters were Li_nO, but Li_nC and a small quantity of Li_n were also present. The production of Li_nC was ascribed to the presence of C in the target material. To process the material into thin metal disks, the Li was rolled in oil and afterwards cleaned with ethanol; thus the Li metal was doped with C compounds. The relative amount of Li_nC with respect to Li_nO was found to vary from run to run; sometimes Li_nC was even more abundant than Li_nO especially for Li_6C and Li_7C (see Fig. 1). We restrict the discussion to measurements on Li_nC clusters with $n \leq 10$ in this paper.

The IP were measured by threshold photoionization spectroscopy using laser light in the 225 nm (5.5 eV) to 400 nm (3 eV) wavelength range, provided by an optical parametric oscillator and a dye laser system; in addition, we used ArF excimer laser radiation at 193 nm (6.4 eV) [16]. Mass abundance spectra were registered as a function of photon energy in steps of 0.04 eV. The signal intensity was obtained by integrating the counts in an interval of about 0.8 amu around the peak maxima. Intensity

[a] Corresponding author.
e-mail: peter.lievens@fys.kuleuven.ac.be

[b] *Present address*: Departamento de Química Orgánica, Universidade de Santiago de Compostela, 15706 Santiago de Compostela, Spain

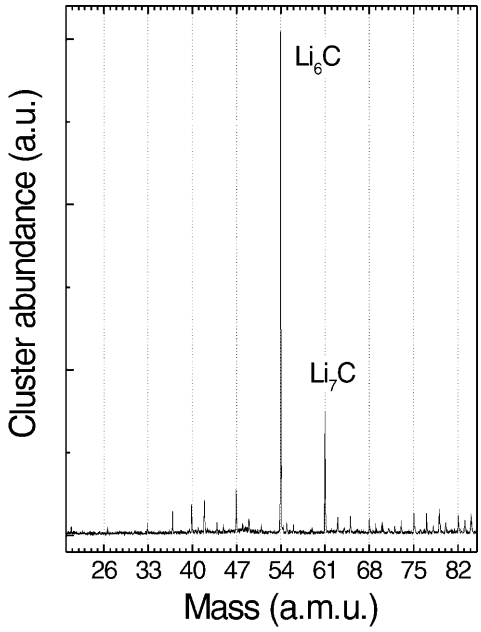

Fig. 1. Time-of-flight mass spectrum of Li_nC clusters.

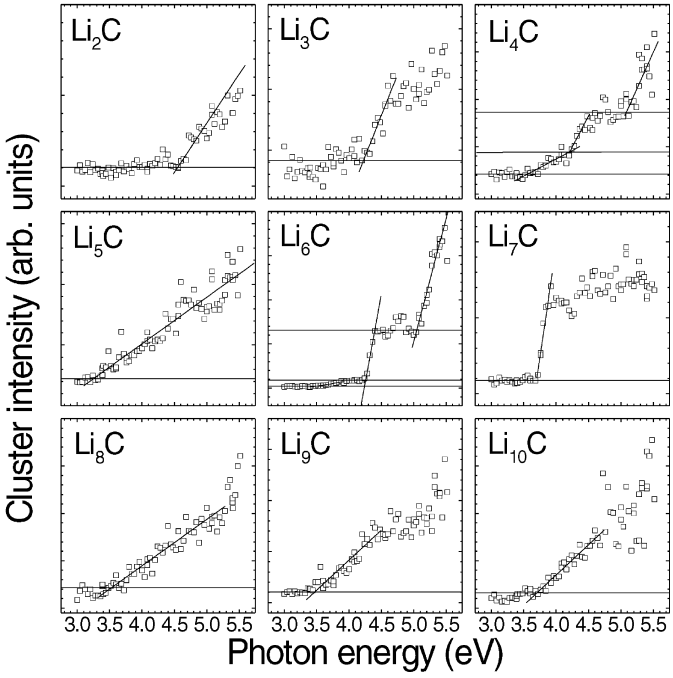

Fig. 2. Photoionization efficiency curves for Li_nC ($n = 2-10$).

fluctuations were reduced by accumulating 2000 production cycles. Long-term production fluctuations were taken into account by the normalization of the abundance spectra, with reference spectra of clusters ionized with photons of 6.4 eV; tunable and reference laser light were sequentially allowed to access the ionization region for typically 20 pulses. Photoionization efficiency (PIE) curves were obtained by plotting the normalized intensity as a function of laser photon energy for each cluster size.

In Fig. 2, the threshold curves are given for Li_nC ($n = 2-10$). To extract values for the IPs, we determined the ionization thresholds by linear extrapolation of the first increase in the PIE curves. This results in the values given in Table 1. In most cases a clear threshold is visible, although the limited production yield leads to a substantial statistical error (about 0.2 eV, see Table 1) in the threshold determination. Li_6C is very particular; apart from an abrupt onset at 4.25 eV, another steep increase of the cluster yield begins at 5.05 eV. Also, a very small ionization probability is noticed below the threshold at 4.25 eV. Similar behavior is observed for Li_4C. It is not obvious how such small ionization signals should be interpreted. These might correspond to Franck–Condon limited ionization into an ionic structure very different from the ground state, but this is not predicted by theory. Several other possible causes can be supposed: multi-photon ionization, fragmentation processes, or the presence of metastable neutral clusters in the beam. Theoretically, we found no indication for low-lying neutral cluster isomers, nor for alternative ionic ground-state structures (see discussion). Experimentally, the laser fluence used for ionization was kept below 100 $\mu J/cm^2$, making multiphoton ionization and fragmentation processes of larger clusters unlikely (but not impossible). IP values extracted from the different slopes in the PIE curves are given in Table 1 for both Li_4C and Li_6C.

3 Calculations

Structures of the smaller clusters (Li_nC and Li_nC^+ ($n \leq 8$)) were optimized employing DFT with the B3LYP [17,18] hybrid functional and the 6-311+G* basis set [19]. Calculations of the harmonic frequencies of the stationary points determined the nature of the stationary points as either minima or saddle points, and gave zero-point vibrational energies (ZPE) (no scaling factor was applied). The vertical ionization potentials (vIP) were obtained by single-point calculations of the ions on the optimized geometries of the neutral species. The adiabatic ionization potential (aIP) is the difference in energy between the optimized structures of neutral and cationic clusters, including the ZPE corrections. In order to obtain more accurate values for the calculated IPs, coupled cluster CCSD(T) [20] and MP4SDTQ [21,22] single points were computed using a larger 6-311+G(2df) [19] basis set, which incorporates higher angular momentum functions. Since the HF wave function suffered from strong spin contamination in some cases, values of the ionization potentials after spin projection (PMP4SDTQ) [23], until [S+3] multiplicity, also are reported when necessary. All calculations employed the Gaussian 94 program package [24]. The results are summarized in Table 2, and the structures are shown in Fig. 3. Calculated IPs are included in Table 1.

4 Discussion of experimental and calculated ionization potentials

Larger Li clusters containing an electronegative atom (as C or O) are best interpreted as almost fully ionic species

Table 1. Calculated and experimental ionization potentials of Li_nC ($n = 2 - 10$).

Species	vIP (eV)	aIP (eV)	exp. IP (eV)
Li_2C	$5.39^a, 5.06^b, 4.92^c, 4.97^d ({}^3A_2 \rightarrow {}^4A_2)$ $5.09^a, 4.54^b, 3.97^c, 4.07^d ({}^3\Sigma_g^- \rightarrow {}^4\Sigma_u^-)$	5.05^a	4.55(20)
Li_3C	$4.55^a, 4.33^b, 3.82^c, 4.14^d ({}^2A_2'' \rightarrow {}^3E)$	4.36^a	4.22(30)
Li_4C	$4.52^a, 5.05^c, 4.97^d ({}^1A_1 \rightarrow {}^2E)$	4.30^a	3.57(20) 4.24(20) 5.09(20)
Li_5C	$3.91^a ({}^2A_1 \rightarrow {}^1A_1)$	3.90^a	3.24(20)
Li_6C	$4.25^a ({}^1A_{1g} \rightarrow {}^2A_{1g})$	4.25^a	3.51(20) 4.25(20) 5.05(20)
Li_7C	$3.78^a ({}^2A_1 \rightarrow {}^1A_1)$	3.78^a	3.69(10)
Li_8C	$4.12^a ({}^1A_{1g} \rightarrow {}^2A_{1u})$	4.07^a	3.53(20)
Li_9C			3.47(20)
$Li_{10}C$			3.62(10)

[a] B3LYP/6-311+G*; [b] CCSD(T)/6-311+G(2df);
[c] MP4SDTQ/6-311+G(2df); [d] PMP4SDTQ/6-311+G(2df).

Table 2. Absolute energies of neutral and cationic Li_nC clusters.

Species	Cluster	Energy (−a.u)[a]	$\langle S^2 \rangle$[b]	ZPE[c]	State
Li_2C	**1**	52.98437	2.511	6.74	${}^3A_2(C_{2v})$
	2	52.99446	2.034	9.40	${}^3\Sigma_g^-(D_{\infty h})$
Li_3C	**6**	60.55211	0.781	14.29	${}^2A_2''(D_{3h})$
Li_4C	**9**	68.12714	0	21.57	${}^1A_1(T_d)$
Li_5C	**11**	75.68672	0.772	27.06	${}^2A_1(C_{4v})$
	13	75.68643	0.773	25.54	${}^2A_1'(D_{3h})$
Li_6C	**15**	83.25099	0	32.94	${}^1A_{1g}(O_h)$
Li_7C	**17**	90.76597	0.759	34.99	${}^2A_1(C_{3v})$
	19	90.75068	0.874	32.72	${}^2B_2(C_{2v})$
Li_8C	**21**	98.29369	0	38.75	${}^1A_{1g}(D_{3d})$
Li_2C^+	**3**	52.80819	3.754	7.42	${}^4\Sigma_u^-(D_{\infty h})$
	4	52.78770	0.752	9.09	${}^2\Pi_u(D_{\infty h})$
	5	52.78369	1.755	7.36	${}^2\Sigma_u^-(D_{\infty h})$
Li_3C^+	**7**	60.39153	0	13.64	${}^3B_1(C_{2v})$
	8	60.39129	0	13.09	${}^3A_2(C_{2v})$
Li_4C^+	**10**	67.96866	0.758	20.63	${}^2B_2(D_{2d})$
Li_5C^+	**12**	75.54329	0	28.06	${}^1A_1(C_{4v})$
	14	75.54390	0	28.03	${}^1A_1'(D_{3h})$
Li_6C^+	**16**	83.09481	0.758	32.47	${}^2A_{1g}(O_h)$
Li_7C^+	**18**	90.62771	0	36.53	${}^1A_1(C_{3v})$
	20	90.60732	0	33.74	${}^1A_1'(C_{2v})$
Li_8C^+	**22**	98.14370	0.768	37.84	${}^2A_{1u}(D_{3d})$

[a] B3LYP/6-311+G* energy;
[b] Expectation value of the squared spin angular moment;
[c] Unscaled zero-point energy (ZPE) in kJ/mol.

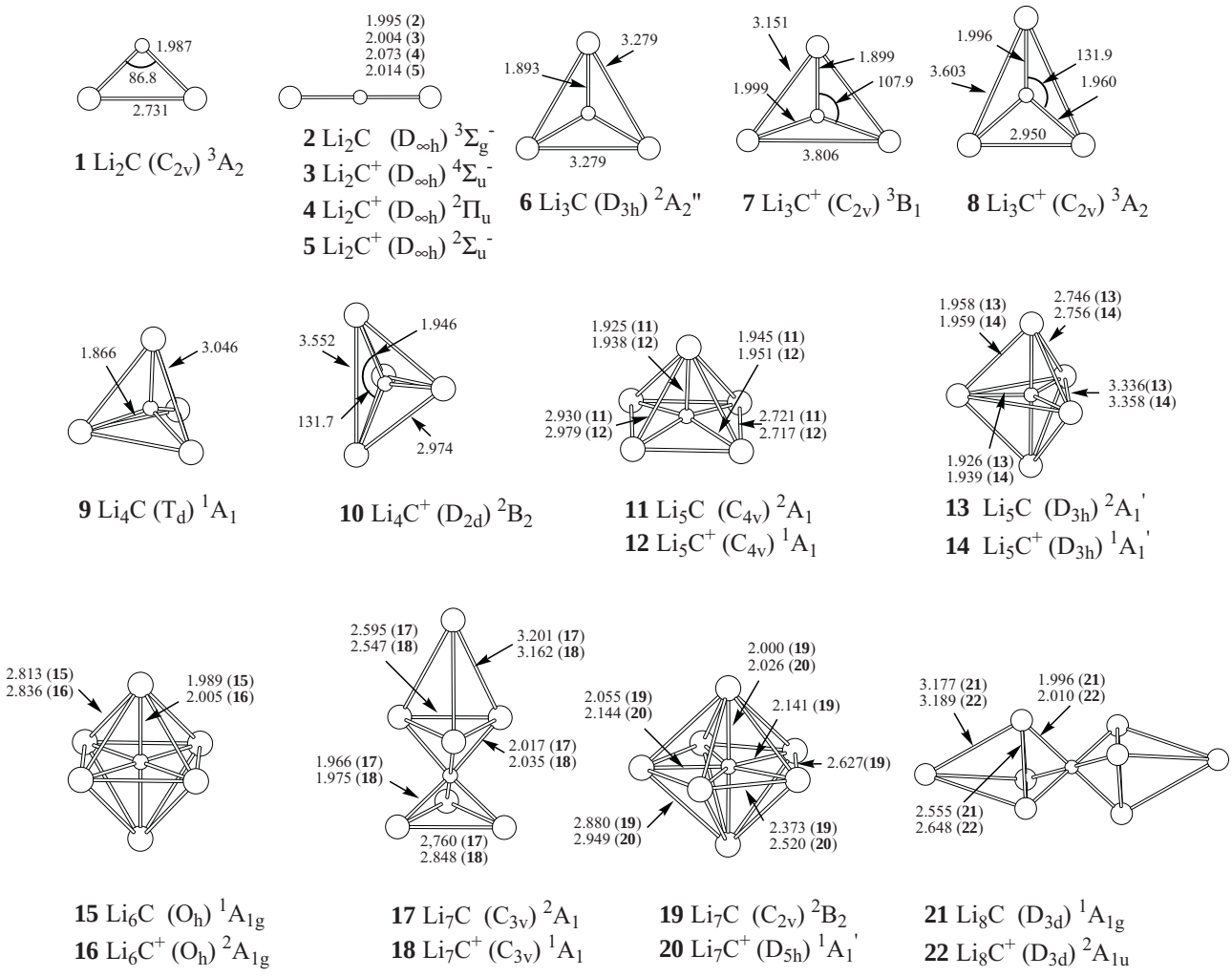

1 Li_2C (C_{2v}) $^3A_2$
2 Li_2C $(D_{\infty h})$ $^3\Sigma_g^-$
3 Li_2C^+ $(D_{\infty h})$ $^4\Sigma_u^-$
4 Li_2C^+ $(D_{\infty h})$ $^2\Pi_u$
5 Li_2C^+ $(D_{\infty h})$ $^2\Sigma_u^-$
6 Li_3C (D_{3h}) $^2A_2"$
7 Li_3C^+ (C_{2v}) $^3B_1$
8 Li_3C^+ (C_{2v}) $^3A_2$
9 Li_4C (T_d) $^1A_1$
10 Li_4C^+ (D_{2d}) $^2B_2$
11 Li_5C (C_{4v}) $^2A_1$
12 Li_5C^+ (C_{4v}) $^1A_1$
13 Li_5C (D_{3h}) $^2A_1'$
14 Li_5C^+ (D_{3h}) $^1A_1'$
15 Li_6C (O_h) $^1A_{1g}$
16 Li_6C^+ (O_h) $^2A_{1g}$
17 Li_7C (C_{3v}) $^2A_1$
18 Li_7C^+ (C_{3v}) $^1A_1$
19 Li_7C (C_{2v}) $^2B_2$
20 Li_7C^+ (D_{5h}) $^1A_1'$
21 Li_8C (D_{3d}) $^1A_{1g}$
22 Li_8C^+ (D_{3d}) $^2A_{1u}$

Fig. 3. Calculated structures of Li_nC and Li_nC^+. Bond distances are given in Å and bond angles in degrees.

in which the C or O attracts charge until its octet is filled. This description is strongly supported by the discontinuities in the IP observed at $n = 10$, 22, and 42, for Li_nO, and at $n = 24$ and 44 for Li_nC [14–16]. These steps are consistent with cluster shell model descriptions if one assumes that O "localizes" two and four Li atoms in a "molecular part". The remaining Li valence electrons are delocalized in the "metallic part" of the cluster.

Due to this highly ionic character, Li_nC clusters from $n = 5$ or more appear to violate the octet rule: five, six, and even higher coordinations of C are found in Li_nC clusters [3, 5]. However, after the C octet is filled, the remaining valence electrons are involved in the Li–Li bonding. For the size range considered in this paper, very small IPs were observed for the C-doped clusters, in contrast to the slowly decreasing trend for pure Li_n from the atomic IP towards the bulk work function [25].

In the following, the experimental results are compared to the calculated structures and IPs for Li_nC ($n = 2 - 8$). Although multicoordinated structures are also expected for Li_9C and $Li_{10}C$ [6], these species were not investigated theoretically in the present study.

4.1 Li_2C

It has been reported elsewhere that the carbene Li_2C has several states close in energy [26]. The lowest forms are the angular $^3A_2$ (**1**) and the linear $^3\Sigma_g^-$ (**2**) states (bold arabic numbers refer to the structures shown in Fig. 3). At the B3LYP/6-311+G* level, the latter is favored by 0.25 eV. However, single-point CCSD(T)/6-311+G(2df) calculations reduced this difference (when the B3LYP ZPE correction is taken into account) to 0.05 eV. Charge analysis following Bader´s Atoms in Molecules (AIM) method [27] gave a higher negative charge for C in the $^3\Sigma_g^-$ state than in the $^3A_2$ state (-1.68 vs. -1.48). Since the Li–Li distance is 2.731 Å in the angular form, this difference in ionic character is due to the presence of some degree of bonding between Li atoms (AIM bond order is only 0.086). Other states studied at the B3LYP level are higher in energy and not relevant for our experiments.

The vIP at the B3LYP level were computed to be 5.39 eV and 5.09 eV for the $^3A_2 \rightarrow {}^4A_2$ and $^3\Sigma_g^- \rightarrow {}^4\Sigma_u^-$ transitions, respectively. CCSD(T) single-point calculations gave lower values (5.06 and 4.54 eV). The latter is

in excellent agreement with experiment and supports $^3\Sigma_g^-$ as the preferred state of the Li_2C carbene. (MP4/ and PMP4/6-311+G(2df) calculations yielded lower values, although they were slightly higher after spin projection; see Table 1.)

We found three linear states for the ionized carbene Li_2C^+: the $^4\Sigma_u^-$ quartet (**3**) and the two doublets, $^2\Pi_u$ (**4**) and $^2\Sigma_u^-$, (**5**) which are 0.58 and 0.67 eV above the quartet form respectively. Charge analysis of the quartet state revealed its highly ionic character (the C charge is −0.87). Consequently, the electrostatic repulsion between the positively charged Li atoms is larger than in the neutral case. This favors the linear geometry of the cation. The calculated B3LYP aIP is 5.05 eV, close to the vIP.

4.2 Li_3C

The substoichiometric Li_3C and Li_3C^+ molecules have been computed previously, first by Chandrasekhar *et al.* [8, 28]. Our B3LYP calculations also gave a trigonal structure with D_{3h} symmetry (**6**) for the lowest state ($^2A_2''$) of the Li_3C radical. The computed vIP, 4.55 eV at the B3LYP level, is in rather good agreement with our 4.22(30) eV experimental IP and the value previously reported by Wu and Ihle (4.6(3) eV) [29]. These all are lower than Kudo´s (5.3(3) eV) [30]. Unrestricted CCSD(T) and MP4SDTQ calculations gave 4.33 and 3.82 eV respectively. While the coupled cluster calculations on Li_3C suffered from strong spin contamination of the reference wave function, the values obtained after spin projection, e.g., 4.14 eV (PMP4SDTQ), again are in good agreement with experiment.

The Li_3C^+ cation has a triplet ($^3B_1$) state with C_{2v} symmetry (**7**) due to Jahn–Teller distortion. Frequency analysis shows the other triplet C_{2v} ($^3A_2$) form (**8**) reported in [28] to be a first-order transition structure between the $^3B_1$ forms, only sligthly higher in energy (0.007 eV without ZPE correction). The wave function of the cation is a mixing of these two states at the neutral geometry employed for the vIP computation. The B3LYP-calculated aIP is lower than the vIP (4.36 vs. 4.55 eV) due to the significant Li–C bond lengthening that occurs in the transition to the equilibrium structure of the cation.

4.3 Li_4C

The Li_4C molecule is known to have a tetrahedral structure (**9**) [3, 4, 8] which can be considered as a C(4−) tetraanion surrounded by four positively charged Li atoms, which form a metal cage. Several slopes are observed in the PIE curve of Li_4C. A slow increase is observed from about 3.5 eV, and two pronounced slopes start at 4.24 and 5.09 eV. These values are very different from an IP reported earlier by Kudo (8.2(3) eV) [30].

The lowest calculated vIP, 4.52 eV at B3LYP/6-311+G*, is very close to the second experimental value (4.24(20) eV). MP4SDTQ/6-311+G(2df) single points gave somewhat higher values of 5.05 eV or 4.97 eV with spin projection[1]. Since the stability of wave functions was checked, these data should correspond to the first ionization potential. A possible explanation for the 3.57(20) eV may be the photofragmentation of larger clusters, rather than direct photoionization. However, this process seems not to be easy, since Li_4C and Li_4C^+ bind Li with an energy of 1.80 and 2.21 eV, respectively. Binding energies of small lithium clusters (Li_2 to Li_4) are even greater. We frankly do not yet have a clear explanation for the origin of the first slope. The slope at 5.09 eV could be due to the existence of low-lying electronic states in Li_4C^+.

The preferred geometry of Li_4C^+ is a D_{2d} Jahn–Teller distorted tetrahedron (**10**); this gives an aIP of 4.30 eV.

4.4 Li_5C

As mentioned above, Li_5C is the smallest hyperlithiated cluster [3, 8]. The most stable geometry is a C_{4v} square pyramid (**11**) in which the C atom is bound directly to five Li atoms. Experimentally, Li_5C shows only one slope in the PIE curve, yielding an IP of 3.24(20) eV; this is lower than the computed value (3.91 eV).

The Li_5C^+ cation prefers a D_{3h} trigonal bipyramid structure (**14**). The aIP (3.90 eV) is close to the vIP, since there is no large change in geometry. These molecules undergo fast pseudo-rotation processes, since the saddle points (**12**) and (**13**) are only 0.008 and 0.017 eV (without ZPE correction) above the corresponding minima.

The large decrease of the IP from Li_4C to Li_5C is easy to understand. A bonding electron in Li_4C must be removed from the central charged C(4−) atom, but for Li_5C, the electron is taken from a weakly bound orbital involving the external Li atoms. In contrast to traditional two-center two-electron bonds, the "extra" electron in Li_5C can be removed more easily, since it plays a minor role in the bonding. The stability of Li_5C is mainly due to the electrostatic attraction between positively charged Li and C(4−). In fact, Li_5C has the smallest IP of all the Li_nC clusters investigated. Metal–metal bonding is more important for the stability of the larger clusters.

4.5 Li_6C

The Li_6C molecule [3, 7, 8, 11, 12, 31, 32] has a remarkable octahedral O_h structure (**15**); the carbon is surrounded by six Li atoms. This molecule is by far the most abundant species observed in the experiment, so six appears to be the preferred coordination number of polylithiated C. The prominence of Li_7C, which also is hexacoordinated, provides additional evidence for the preference for this coordination number in C-doped Li clusters. (See, however, [6]).

[1] CISD calculations (which involve single and double excitations from the reference determinant) on Li_4C and Li_4C^+ do not show a significant multireference character for these molecules, which should therefore be described reasonably well by calculations based on one determinant.

The experimental spectrum has two pronounced slopes corresponding with IPs of 4.25(20) and 5.05(20) eV. The value of 4.25 eV is the highest of all the hyperlithiated monocarbide clusters, in agreement with the high thermodynamic stability of Li_6C. The computed vIP is lowest for the $^1A_{1g} \rightarrow {}^2A_{1g}$ transition (4.25 eV at B3LYP/6-311+G*) and is in perfect agreement with the IP deduced from the most pronounced slope in the PIE curve (4.25 eV). We performed CIS/6-311+G* single-point calculations [33] on the B3LYP geometry of the neutral form in Li_6C^+, showing the existence of an excited state (whose density breaks molecular symmetry) at 1.40 eV. This may account for the second pronounced slope in the spectrum.

As for Li_4C, some ionization probability is seen, starting from about 3.5 eV. This low IP value is not reproduced by theory (wave-function stability was checked). A possible reason could be the fragmentation of larger clusters, which is strongly supported by the thermodynamic stability of Li_6C. In fact, Li_7C and Li_8C and their corresponding ions have quite low fragmentation energies, as is shown by the following dissociations:

$$Li_7C \rightarrow Li_6C + Li \qquad \Delta H^{0K} = 0.62\,eV (60.0\,kJ/mol)$$
$$Li_7C^+ \rightarrow Li_6C^+ + Li \qquad \Delta H^{0K} = 1.09\,eV (105.1\,kJ/mol)$$
$$Li_8C \rightarrow Li_6C + Li_2 \qquad \Delta H^{0K} = 0.69\,eV (66.8\,kJ/mol)$$
$$Li_8C^+ \rightarrow Li_6C^+ + Li_2 \qquad \Delta H^{0K} = 0.86\,eV (83.5\,kJ/mol)$$

The aIP of Li_6C (4.25 eV) is very close to the vIP, since only a tiny increase in bond lengths is observed in Li_6C^+ (**16**) with respect to the neutral form (**15**).

4.6 Li_7C

The most stable form of the Li_7C molecule is computed to be a C_{3v} structure (**17**) which results when one face of the octahedral Li_6C is capped with another Li atom. This structure is a minimum both for the neutral doublet and the cationic singlet (**18**) states. Among higher coordinated structures, we found a C_{2v} pentagonal bipyramid (**19**) (a Jahn–Teller distortion of a D_{5h} pentagonal bipyramid). For Li_7C^+, this form (**20**) has the full D_{5h} symmetry. These heptacoordinated forms are higher in energy by 0.39 and 0.52 eV for the neutral and the cationic species, respectively.

The PIE curve has a well-defined slope, with a baseline intercept at 3.69(10) eV. Our calculated vIP for the C_{3v} structure (**17**) is 3.78 eV, which is in good agreement with experiment. The calculated vIP for the heptacoordinated form (**19**) is somewhat higher: 3.97 eV. This can be attributed to a larger increase in electrostatic repulsion between the positively charged Li atoms in the more compact heptacoordinated form.

The calculated aIP is 3.78 eV, identical to the vIP. The principal difference between the neutral and charged C_{3v} forms is the decrease of bond lengths in the Li-capped face and an increase in distances in the opposite face. Hence, the electronic density is removed mainly from the non-capped face.

4.7 Li_8C

Marsden *et al.* [5, 6] have proposed the most stable structure of Li_8C to be D_{3d} (**21**), with a hexacoordinated carbon, and two faces of the octahedron capped by Li atoms. Our calculations on this structure gave a vIP of 4.12 eV. As for Li_7C, there are only small changes in geometry between the neutral and cationic forms (**22**); the computed aIP is 4.07 eV. The vIP value is quite different from experiment (3.53(20) eV). The existence of other Li_8C isomers or Li_8C^+ states cannot be excluded, although Marsden's alternative D_{2d} Li_8C form was appreciably higher in energy [6].

5 Conclusions

We investigated the ionization potentials of C-doped Li clusters experimentally, by threshold photoionization spectroscopy, and theoretically, by density functional theory. In general, the quantitative agreement between the measured and calculated IPs is satisfactory, especially in view of the expected systematic inaccuracy usually encountered in the determination of the IPs from PIE curves. Furthermore, the appearance of several distinct slopes in the PIE curves could be at least partially accounted for theoretically as transitions between excited neutral and ionic cluster states. Finally, the high production yield for the hexacoordinated and hypervalent clusters, Li_6C and Li_7C, which is due to their high thermodynamic stability, should allow future investigations of the optical absorption properties.

We thank Dr.H. Bettinger for his help with the coupled cluster calculations. This project is financially supported by the Fund for Scientific Research – Flanders (Belgium) (F.W.O), by the Flemish Concerted Action (G.O.A.) Research Programme, and the Interuniversity Poles of Attraction Programme – Belgian State, Prime Minister's Office – Federal Office for Scientific, Technical and Cultural Affairs (I.U.A.P.). The work at Erlangen was supported by the Deutsche Forschungsgemeinschaft (DFG) and the Fonds der Chemischen Industrie. P.L. is a Postdoctoral Researcher of the F.W.O. W.B. thanks the Flemish Institute for Scientific-Technological Research (I.W.T.) for financial support. H.W. is a Postdoctoral Researcher of the European Community Training and Mobility of Researchers Programme (T.M.R.). A.N. acknowledges the University of Santiago de Compostela for a study fellowship.

References

1. C.H. Wu, H. Kudo, H.R. Ihle: J. Chem. Phys. **70**, 1815 (1979)
2. P.v.R. Schleyer, E.-U. Würthwein, J.A. Pople: J. Am. Chem. Soc. **104**, 5839 (1982)
3. P.v.R. Schleyer, E.-U. Würthwein, J.A. Pople: J. Am. Chem. Soc. **105**, 5930 (1983)
4. P.v.R. Schleyer: in *New Horizons of Quantum Chemistry*, ed. by P.O. Löwdin, B. Pullman (D. Reidel Publ., Dordrecht 1983) p. 95

5. J. Ivanic, C.J. Marsden, D.M. Hasset: J. Chem. Soc. Chem. Commun. 822 (1993)
6. J. Ivanic, C.J. Marsden: J. Am. Chem. Soc. **115**, 7503 (1993)
7. P.v.R. Schleyer, J. Kapp: Chem. Phys. Lett. **225**, 363 (1996)
8. W. Zhizhong, Z. Xiange, T. Auchin: J. Mol. Struct. (Theochem) **453**, 225 (1998), and reference therein
9. V.G. Zakrzewski, W. von Niessen, A.I. Boldyrev, P.v.R. Schleyer: Chem. Phys. Lett. **197**, 195 (1992), and refereces therein
10. R.O. Jones, A.I. Lichtenstein, J. Hutter: J. Chem. Phys. **106**, 4566 (1997), and references therein
11. P.v.R. Schleyer, A. Streitwieser: in *Bonding, Structures and Energies in Organolithium Compounds*, ed. by A.M. Sapse, P.v.R. Schleyer (Wiley, New York 1995)
12. H. Kudo: Nature **355**, 432 (1992)
13. R.G. Parr, W. Yang: *Density Functional Theory of Atoms and Molecules* (Univ. Press, Oxford 1989)
14. P. Lievens, P. Thoen, S. Bouckaert, W. Bouwen, F. Vanhoutte, H. Weidele, R.E. Silverans, A. Navarro-Vázquez, P.v.R. Schleyer: J. Chem. Phys. **110**, 10 316 (1999)
15. P. Lievens, P. Thoen, S. Bouckaert, W. Bouwen, F. Vanhoutte, H. Weidele, R.E. Silverans: Chem. Phys. Lett. **302**, 571 (1999)
16. P. Lievens, P. Thoen, S. Bouckaert, W. Bouwen, E. Vandeweert, F. Vanhoutte, H. Weidele, R.E. Silverans: Z. Phys. D **42**, 231 (1997)
17. C. Lee, W. Yang, R.G. Parr: Phys. Rev. B **37**, 785 (1988)
18. A.D. Becke: J. Chem. Phys. **98**, 5648 (1993)
19. W. Hehre, L. Radom, P.v.R. Schleyer, J.A. Pople: *Ab initio Molecular Orbital Theory* (Wiley, New York 1986)
20. J.A. Pople, M. Head-Gordon, K. Raghavachari: J. Chem. Phys. **87**, 5968 (1987)
21. R. Krishnan, J.A. Pople: Int. J. Quantum Chem. **14**, 91 (1978)
22. R. Krishnan, M.J. Frisch, J.A. Pople: J. Chem. Phys. **72**, 4244 (1980)
23. H.B. Schlegel: J. Phys. Chem. **92**, 3075 (1988)
24. Gaussian 94, Revision E.2, M.J. Frisch, G.W. Trucks, H.B. Schlegel, P.M.W. Gill, B.G. Johnson, M.A. Robb, J.R. Cheeseman, T. Keith, G.A. Petersson, J.A. Montgomery, K. Raghavachari, M.A. Al-Laham, V.G. Zakrzewski, J.V. Ortiz, J.B. Foresman, J. Cioslowski, B.B. Stefanov, A. Nanayakkara, M. Challacombe, C.Y. Peng, P.Y. Ayala, W. Chen, M.W. Wong, J.L. Andres, E.S. Replogle, R. Gomperts, R.L. Martin, D.J. Fox, J.S. Binkley, D.J. Defrees, J. Baker, J.P. Stewart, M. Head-Gordon, C. Gonzalez, J.A. Pople: Gaussian, Inc., Pittsburgh, PA, 1995
25. Ph. Dugourd, D. Rayane, P. Labastie, B. Vezin, J. Chevaleyre, M. Broyer: Chem. Phys. Lett. **197**, 433 (1992); B. Vezin, J. Chevaleyre, M. Broyer: Surf. Rev. Lett. **3**, 171 (1996)
26. A. Mavridis, J.F. Harrison: J. Am. Chem. Soc. **104**, 3827 (1982)
27. R.F.W. Bader: *Atoms in Molecules: A Quantum Theory* (Univ. Press, Oxford 1990)
28. J. Chandrasekhar, J.A. Pople, R. Seeger, U. Seeger, P.v.R. Schleyer: J. Am. Chem. Soc. **104**, 3651 (1982)
29. C.H. Wu, H.R. Ihle: Chem. Phys. Lett. **61**, 54 (1979)
30. H. Kudo: Chem. Lett. **9**, 1611 (1989)
31. A.E. Reed, F. Weinhold: J. Am. Chem. Soc. **107**, 1919 (1985)
32. J.P. Ritchie, S.M. Bachrach: J. Am. Chem. Soc. **109**, 5909 (1987)
33. J.B. Foresman, M. Head-Gordon, J.A. Pople, M.J. Frisch: J. Chem. Phys. **96**, 135 (1992)